COMMUNICATION

Dynamical Evolution of the 2D/3D Interface: A Hidden Driver behind Perovskite Solar Cell Instability

Received 00th January 20xx,
Accepted 00th January 20xx

DOI: 10.1039/x0xx00000x

Albertus A. Sutanto,[a] Nikita Drigo,[a] Valentin I. E. Queloz,[a] Inés Garcia Benito,[a] Ahmad R. Kirmani,[bc] Lee J. Richter,[b] Pascal A. Schouwink,[d] Kyung Taek Cho,[a] Sanghyun Paek,[a] Mohammad Khaja Nazeeruddin,*[a] Giulia Grancini*[a,e]

Engineering two-/three- dimensional (2D/3D) perovskite solar cells is nowadays a popular strategy for efficient and stable devices. However, the exact function of the 2D/3D interface in controlling the long-term device behavior is still obscure. Here, we reveal a dynamical structural mutation of the 2D/3D interface: the small cations in the 3D cage move towards the 2D layer, which acts as an ion scavenger. If structurally stable, the 2D physically blocks the ion movement at the interface boosting the device stability. Otherwise, the 2D embeds them, dynamically self-transforming into a quasi-2D structure. The judicious choice of the 2D constituents is decisive to control the 2D/3D kinetics and improve the device lifetime, opening a new avenue for perovskite interface design.

Introduction

Within the last decade, perovskite solar cells (PSC) have been receiving a great interest in the area of new generation photovoltaics, with power conversion efficiency (PCE) recently surpassing 25%.[1] Careful interface engineering between the perovskite active layer (AL) and the device interfaces, i.e. the electron or the hole transporting layers (ETL, HTL), is the key to device development and optimization. Various engineering strategies have been explored, including interface functionalization with bulky organic molecules,[2] inert polymeric layers,[3-5] inorganic interlayers,[6, 7] graphene or parent 2D materials,[8-10] Alternatively, layered perovskites, popularly referred as 2D,[11, 12] have been incorporated at the AL-ETL or-HTL interface, forming graded 2D/3D interfaces.[13-18] Thanks to the superior robustness of the 2D compared to parent 3D perovskite, such 2D/3D architectures have attracted growing interest as a route to stable and efficient devices.[2] For instance, a combination of methylammonium (MA) lead iodide perovskites and aminovaleric acid-based 2D resulted in solar cells with greater than 1-year stability, demonstrating the robust nature of the combined systems.[19] The 2D perovskite has been shown to simultaneously function as a protective layer and surface defect passivant.[17, 20, 21] However, whether 2D is an essential ingredient for future PSC technology or a popular transitory trend is an open question.[22, 23] To answer this point, it is imperative to understand how the 2D perovskite affects the quality of the 3D perovskite surface, and the processes therein, as well as the ultimate device behavior, performance and stability over time.

Here, we report the observation of a slow evolution of the performance of 2D/3D PSCs using a new family of thiophene alkylammonium-based organic cations as building blocks for the layered 2D perovskites and its impact on the device efficiency and stability. We reveal a double effect: First, unexpectedly, during aging for several months in dark and dry environment, the PSC efficiency increases (from 15% to over 20% in the most striking case), mainly associated with an enhancement of the device open circuit voltage (Voc). While this stems true also for the controller device, a significant boost is observed as derived from a slow structural rearrangement of the 2D/3D interface. We attribute this to the "soft" nature of the 2D perovskite overlayer that can act as an ion-scavenger. As a consequence of ion movement from the 3D towards the interface, small MA cations accumulate at the interface. As a getter, the 2D structure can incorporate the MA cations by self-modifying its pure layered structure into a quasi-2D (or mixed) phase.[11] This interface modification generally improves the device performance. On the other side, depending on the chemical nature of the 2D perovskite, a "more robust" 2D layer can prevent such structural change, physically blocking the ion

[a] Group for Molecular Engineering of Functional Materials, Institute of Chemical Sciences and Engineering, École Polytechnique Fédérale de Lausanne (EPFL), Valais Wallis, Rue de l'Industrie 17, CH-1951 Sion, Switzerland. E-mail: mdkhaja.nazeeruddin@epfl.ch
[b] Materials Science and Engineering Division, National Institute of Standards and Technology (NIST), Gaithersburg, MD, 20899 USA.
[c] Guest Researcher @ Materials Science and Engineering Division, National Institute of Standards and Technology (NIST), Gaithersburg, MD, 20899 USA.
[d] Institut des Sciences et Ingénierie Chimiques, École Polytechnique Fédérale de Lausanne, Valais Wallis, CH-1951 Sion, Switzerland
[e] Dipartimento Di Chimica Fisica, University of Pavia, Via T. Taramelli, 14, 27100 Pavia, Italy. E-mail: giulia.grancini@unipv.it
†Electronic Supplementary Information (ESI) available: [details of any supplementary information available should be included here]. See DOI: 10.1039/x0xx00000x

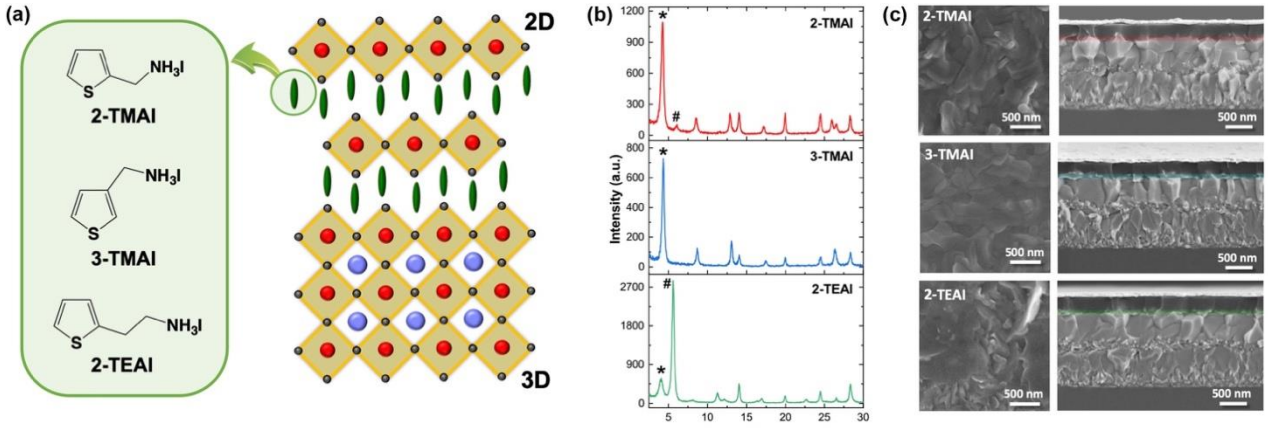

Figure 1. (a) Molecular structures of the cations (left) and sketch (right) of the derived 2D/3D interface. (b) X-ray diffraction (XRD) pattern at 2° incident angle of the 2D/3D film employing 2-TMAI, 3-TMAI and 2-TEAI cations in the 2D template. # and * denote diffraction peaks of 2D perovskite with n=1 and n=2, respectively. (c) Scanning electron microscopy images of the top view (left) of the perovskite films and cross-section (right) of the 2D/3D devices employing 2-TMAI, 3-TMAI and 2-TEAI cations in the 2D layer (highlighted with colored area).

movement. This leads to a dramatic increase in the device stability, retaining 90% of the initial value under continuous illumination over 1000 hours. The structural change in time has been monitored over a time window of months combining solar cell operation with thin film structural and optical characterization on aged samples and/or under different aging conditions (i.e. different thermal stress). Overall, results reveal that the conscious choice of proper 2D components can control the dynamical evolution of the 2D/3D interfaces and is a key element to control for the realization of efficient and stable devices.

Results and discussion

We synthesized a series of bulky thiophene-terminated cations as building blocks for layered 2D perovskite structure. Chemical formulae of the thiophenealkylammonium salts namely 2-thiophenemethylammonium iodide (2-TMAI), 3-thiophenemethylammonium iodide (3-TMAI), and 2-thiopheneethylammonium iodide (2-TEAI) along with the derived 2D structure are shown in Figure 1a. Notably, they only differ on position and length of the alkyl chain connecting the thiophene core and the ammonium entity. The salts were prepared from the commercially available amines and HI (see Supporting Information for details).

To create the 2D/3D thin films and devices, we dissolved the salts in isopropanol (IPA) and dynamically spin-coated them on top of a triple-cations $[(FAPbI_3)_{0.87}(MAPbBr_3)_{0.13}]_{0.92}(CsPbI_3)_{0.08}$ based 3D perovskite film, where FA stands for formamidinium (see Supporting Information for details). As a result, a thin layer of 2D perovskite is formed on top of the 3D bulk, as verified by low angle grazing incidence X-Ray Diffraction (XRD). Patterns are shown in Figure 1b. We note the presence of the peaks at 14°, and at 6° and 4° which correspond to (001) diffraction signals from the 3D perovskite, and, at lower angles, from (002) of the layered 2D perovskites, respectively. (The 2D crystal structures are either centro-symmetric or near centro-symmetric such that the (00l) diffraction, l odd, is forbidden or weak.) More in details, the peak at 6° relates to the formation of a pure 2D perovskite, which takes the formula of $R_2(MA)_{n-1}PbI_{3n+1}$ for n=1 (where n defines the number of the inorganic layers), while the peak at 4° relates to a mixed phase (or Quasi-2D perovskite) where, in this case, n=2. Depending on the organic salts, slightly different 2D perovskites are formed: for 2-TMAI mostly n=2; for 3-TMAI only n=2; and for 2-TEAI mostly n=1 2D phase (see also XRD patterns of the pure 2D perovskite in Figure S1 and S2). The 2D perovskite layer, ≈50 nm thick, covers the entire 3D surface, as shown in Figure 1c by top view and cross-sectional scanning electron microscopy (SEM) images. From the top surface image, we could observe that the 2D overlayer smooths out the surface, rendering it less defined in terms of grain boundaries and crystals borders with respect to the 3D surface (Figure S3).

We implement these films as AL in standard (n-i-p) device structure solar cells (see Supporting Information). The optimized thiophenealkylammonium salts concentration implemented in the devices is 0.06M, resulting in ≈50 nm thick 2D layer on top of 3D layer (see Table S1 for details). The photovoltaic (PV) response of the thiophene-based 2D/3D cells are shown in Figure 2, Table 1 (statistics in Table S2 and Figure S4). It is worth remarking that commonly device data shown in literature do not specify the aging status of the measured device, making the comparison among reported PCE rather difficult. This also hides important information on the slow dynamic behavior of the device interfaces that can alter the PSC performances.[24] Slow processes such as those related to ionic

Table 1. Photovoltaic parameters of champion fresh and aged (for the time as indicated in Figure 2) of 2D/3D PSCs employing 2-TMAI, 3-TMAI, 2-TEAI, and 3D control.

Organic cations		Voc (V)	Jsc (mA cm^{-2})	FF	PCE (%)
2-TMAI	Fresh	1.049	23.75	0.719	17.91
	Aged	1.132	23.50	0.751	**19.97**
3-TMAI	Fresh	1.032	23.67	0.760	18.55
	Aged	1.132	23.60	0.771	**20.59**
2-TEAI	Fresh	1.010	24.01	0.647	15.70
	Aged	1.117	23.60	0.737	**19.42**
3D	Fresh	1.041	23.87	0.765	19.01
	Aged	1.124	23.57	0.773	**20.48**

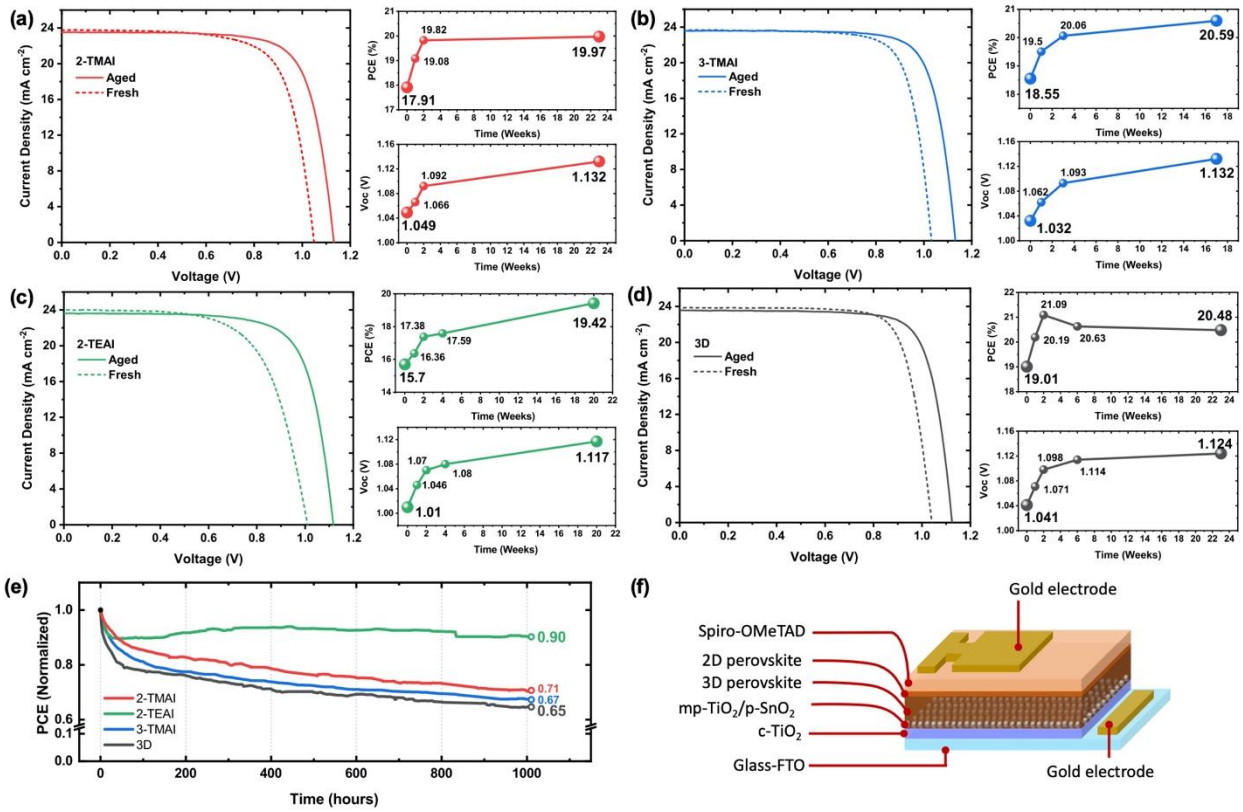

Figure 2. Photovoltaics characteristics of the 2D/3D PSCs employing (a) 2-TMAI, (b) 3-TMAI and (c) 2-TEAI, (d) 3D control. For each panel the current-voltage characteristics of fresh and aged devices are shown along with the time evolution of the power conversion efficiency (PCE) and open circuit voltage (V_{OC}) of the devices stored in the dark and dry environment (humidity <10%). (e) Stability test for freshly prepared devices under continuous 1 sun illumination for 1000 h in Ar atmosphere without any encapsulation. (f) Scheme of the device architecture.

motion are still not yet fully understood[25-27] but pointed as common source of aging phenomena. To address this point, here we monitor the evolution of the devices PV performances by comparing fresh (measured 1 day after device fabrication) and aged devices over months (stored in dark and dry air environment with the humidity controlled below 10%).

Fresh device PCEs range from 15% to 19% depending on the 2D/3D system. For the control it reaches peak performances after 2 weeks resulting in 21.1% PCE, but decreasing afterwards (Figure 2d). On the other side, the 2D/3D systems all show a monotonic improvement in the PCE nearly saturating after 6 months. The aged samples all deliver around 20% PCE with an increase in the device FF and Voc. The 3-TMAI device outperforms the 3D control after aging. Notably, the 2-TEAI 2D/3D systems shows the largest improvement of approx. 25% going from 15.70% to 19.42%. Hysteresis and IPCE spectra are reported in Figure S5 and S6. This represents our first finding: the presence of the 2D layer improves the performances over time on month-base analysis. Notably, the highest performances of the devices (also the controller) are always reached after few days of storage in dark and in dry air. However, it is worth mentioning that the final Voc is higher for the 2D/3D system employing 3-TMAI and 2-TMAI. In agreement with previous work on the 2D/3D interface,[28] this can be associated to a surface passivation effect of the 2D layer. To assess that, we investigated the device characteristics under different sunlight intensity, as shown in Figure S7 and S8 and we find the 2D layer has a beneficial effect on surface recombination. Studies of the device ideality factor, based on the intensity dependence of the Voc (Figure S7) and Jsc (Figure S8) provide insight into the recombination kinetics in the device [29, 30]. Additional interface impedance analysis will be performed to better elucidate the interface recombination channels. Relative to the control, all 2D/3D devices exhibit indeed less monomolecular (trap-mediated) recombination which points toward a reduction of the surface trap density, responsible for the improve in the Voc and FF. A second important observation relates to device stability where a distinct behavior is observed depending on the nature of the 2D cation. In general, the 2D/3D devices only slightly outperform the 3D reference when measured under continuous 1 sun illumination at full maximum power point for 1000 h in an inert atmosphere (Figure 2e) showing, after initial decay as commonly observed for 3D PSCs,[31] a similar degradation curve. Interestingly, the 2-TEAI based 2D/3D device behaves differently: the stability after the initial decay, as commented above, recovers and is kept at 90% of the initial PCE value with no sign of degradation for the 1000 h tested. This represents a net improvement with respect to the controller which decays to 65% of the initial value. To rationalize our finding and elucidate the intimate mechanisms behind such long-term stability, we investigate the evolution in time of the 2D/3D structure by means of photoluminescence (PL) spectral

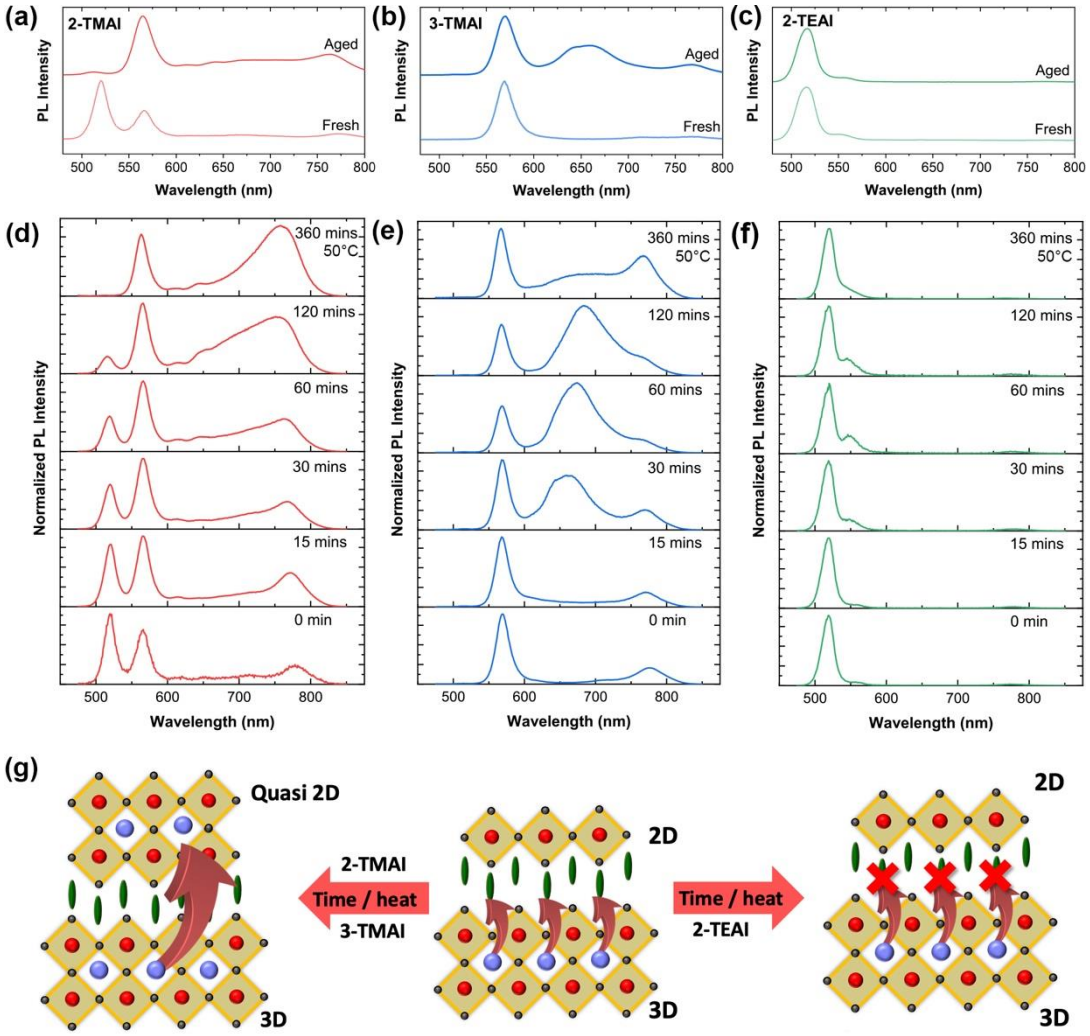

Figure 3. PL spectra upon excitation at 450 nm of fresh and 4 months aged 2D/3D perovskite films employing (a) 2-TMAI, (b) 3-TMAI, and (c) 2-TEAI 2D/3D systems; PL spectra upon thermal stress (heating the film at 50°C for the time as indicated in the legend) for (d) 2-TMAI, (e) 3-TMAI, and (f) 2-TEAI 2D/3D systems. (g) Cartoon illustrating the proposed interfacial mechanism.

analysis as a simple and immediate method to identify the emissive species, and related perovskite phase. PL measurements have been carried out over months, mimicking the same time window as for the device tests, as well as fresh but upon different thermal stress, see Figure 3.

Figure 3a–c shows the PL spectra from the front side (2D perovskite side) of the 2D/3D film exciting both the 2D and the 3D layer for the fresh and aged samples. A weak emission from the 3D perovskite at 770 nm is observed upon front side excitation. Contrarily, upon back side (3D perovskite side) excitation the emission from 3D perovskite is dominant, see Figure S9. For fresh films, peaks at short wavelengths are observed, which manifest at: *1)* 520 nm and 570 nm for 2-TMAI; *2)* 570 nm only for 3-TMAI; *3)* 520 nm (dominant) and a shoulder at 550 nm for 2-TEAI. In agreement with XRD analysis, we can assign the 520 nm PL peak to the emission from n=1 2D perovskite, and the 570 nm peak to n=2 perovskite. This assignment also matches the emission from pure 2D thin films with n=1 or n=2 (see Figure S10 and S11). This indicates the formation of distinct 2D perovskite phases depending on the nature of the organic cations. Upon aging, the emission spectra change: *1)* 520 nm peak (related to n=1 2D) vanishes, while the 570 nm peak grows in 2-TMAI; *2)* the 570 nm is unchanged, but a new broad peak at higher wavelength appears in 3-TMAI. This is related to the formation of a mixed 2D with a higher n value;[11] *3)* 2-TEAI based 2D/3D does not show any visible change. This indicates a structural rearrangement of the 2D/3D interface upon aging that holds true for all cases except for the 2-TEAI-2D/3D thin film. A stable n=1 2D phase upon aging is also observed for PEAI-based 2D/3D systems, confirming the general validity of our observation, see Fig. S12 and S13. Such structural changes are also confirmed by Grazing Incidence Wide Angle X-ray Scattering (GIWAXS) analysis carried out on aged samples, as shown in Figure S14. This observation reveals a structural transformation of the 2D perovskite from a low n to a higher n quasi-2D/3D interface over time for all the cations except the 2-TEAI based 2D/3D.

To better elucidate the origin of this change, we simulate aging by stressing the thin films at 50°C from 0 to 360 minutes and we measure the evolution of the PL spectra over time

(Figure 3d-f). A clear change in the emission peaks position and relative intensity is again observed for the 2-TMAI and 3-TMAI 2D/3D films, while only a minor modification happens for 2-TEAI films. More in detail, for 2-TMAI 2D/3D, the peak at 520 nm reduces in intensity in favor of the peak at 570 nm, vanishing completely after 360 min, while for 3-TMAI 2D/3D, the peak at 570 nm does not change. In both cases, a broad peak at higher wavelength grows. In contrast, for 2-TEAI the 520 nm peak is mostly unaltered (small shoulder at 550 nm appears) and no emission at longer wavelengths is observed. The broad red peak present in 2-TMAI and 3-TMAI can be related to the formation of quasi-2D phase. This result matches with what is observed upon aging, pointing to a similar phenomenon behind such structural changes. It is worth mentioning that the aging does not degrade the 3D bulk underneath, since the absorption spectra of the films do not change (Figure S15) and also the XRD patterns of aged and thermally stressed films show no change in the 3D structures (Figure S16 and S17).

The preceding observations can be explained by the following mechanism as shown in Figure 3g. The 2D perovskite, in case of 2-TMAI and 3-TMAI, functions as a dynamical "sponge" that can embed small ions (such as MA or FA) migrating from the 3D bulk underneath immobilizing them into the new quasi-2D structure. This does not happen for the 2-TEAI 2D/3D that only physically blocks the ion at the interface, preserving the initial purity of the 2D phase (n=1). We can thus infer that the presence of a structurally robust 2D layer (such as in the case of the 2-TEAI) is paramount to control device stability, demonstrating that the purity of the layered 2D structure and its robustness against ion movement and infiltration has crucial impact on the long-term device stability. We can speculate that this intimately relates to the different packing motif of the organic cations dictated by the length of the side alkyl chain which imparts the robustness of the 2D structure. Further work on the structural stability is the focus on ongoing work.

Conclusions

We revealed that 2D/3D interfaces are dynamical in nature, acting as ion-scavengers and self-transforming, upon aging or thermal stress, into quasi-2D graded interfaces. In general, the deposition of 2D layer with various thiophene alkylammonium iodide cations protect the 3D layer from the degradation in the ambient air. This can improve the device performance upon dark aging, but does not lead to stable device operation under illumination. Proper engineering of the 2D/3D system, by judicious choice of the organic cation can lead to structurally stable and robust 2D overlayers (with n=1) that have a decisive role in improving device stability under illumination. A careful molecular design of large organic cation which can maintain the quasi-2D graded interface (n=2) over dark aging and thermal stress is very important to deliver both stable and efficient PSCs. These observations pave the way for new for the development of an intelligent molecular engineering approach to guide smart device design and application of stable 2D/3D interfaces even beyond PVs.

Conflicts of interest

There are no conflicts to declare.

Acknowledgements

This research used the 11-BM(CMS) beamline of the National Synchrotron Light Source II, a U.S. Department of Energy (DOE) Office of Science User Facility operated for the DOE Office of Science by Brookhaven National Laboratory under Contract No. DE-SC0012704. We acknowledge Dr. Ruipeng Li for assistance at the beamline. We acknowledge Professor Raffaella Buonsanti for the use of the Fluorolog system and Dr. Mounir Mensi for fruitful discussion. We acknowledge the Swiss National Science Foundation (SNSF) funding through the Ambizione Energy Project No. 646 HYPER (Grant No. PZENP2173641) and though the Synergia Grant EPISODE (Grant No. CRSII5_171000). G.G. acknowledges the "HY-NANO" project that has received funding from the European Research Council (ERC) Starting Grant 2018 under the European Union's Horizon 2020 research and innovation programme (Grant agreement No. 802862).

Notes and references

1. https://www.nrel.gov/pv/cell-efficiency.html).
2. E. H. Jung, N. J. Jeon, E. Y. Park, C. S. Moon, T. J. Shin, T.-Y. Yang, J. H. Noh and J. Seo, *Nature*, 2019, **567**, 511-515.
3. Q. Wang, Q. Dong, T. Li, A. Gruverman and J. Huang, *Adv. Mater.*, 2016, **28**, 6734-6739.
4. S. H. Turren-Cruz, A. Hagfeldt and M. Saliba, *Science*, 2018, **362**, 449-453.
5. M. Kim, S. G. Motti, R. Sorrentino and A. Petrozza, *Energy Environ. Sci.*, 2018, **11**, 2609-2619.
6. H. Peng, W. Sun, Y. Li, S. Ye, H. Rao, W. Yan, H. Zhou, Z. Bian and C. Huang, *Nano Res.*, 2016, **9**, 2960-2971.
7. N. Arora, M. I. Dar, A. Hinderhofer, N. Pellet, F. Schreiber, S. M. Zakeeruddin and M. Gratzel, *Science*, 2017, **358**, 768-771.
8. A. Agresti, S. Pescetelli, B. Taheri, A. E. Del Rio Castillo, L. Cina, F. Bonaccorso and A. Di Carlo, *ChemSusChem*, 2016, **9**, 2609-2619.
9. P. O'Keeffe, D. Catone, A. Paladini, F. Toschi, S. Turchini, L. Avaldi, F. Martelli, A. Agresti, S. Pescetelli, A. E. Del Rio Castillo, F. Bonaccorso and A. Di Carlo, *Nano Lett.*, 2019, **19**, 684-691.
10. L. Najafi, B. Taheri, B. Martín-García, S. Bellani, D. Di Girolamo, A. Agresti, R. Oropesa-Nuñez, S. Pescetelli, L. Vesce, E. Calabrò, M. Prato, A. E. Del Rio Castillo, A. Di Carlo and F. Bonaccorso, *ACS Nano*, 2018, **12**, 10736-10754.
11. D. H. Cao, C. C. Stoumpos, O. K. Farha, J. T. Hupp and M. G. Kanatzidis, *Journal of the American Chemical Society*, 2015, **137**, 7843-7850.
12. C. C. Stoumpos, D. H. Cao, D. J. Clark, J. Young, J. M. Rondinelli, J. I. Jang, J. T. Hupp and M. G. Kanatzidis, *Chem. Mater.*, 2016, **28**, 2852-2867.
13. K. Yao, X. Wang, F. Li and L. Zhou, *Chem. Commun.*, 2015, **51**, 15430-15433.

14. C. Ma, C. Leng, Y. Ji, X. Wei, K. Sun, L. Tang, J. Yang, W. Luo, C. Li, Y. Deng, S. Feng, J. Shen, S. Lu, C. Du and H. Shi, *Nanoscale*, 2016, **8**, 18309-18314.
15. J. Chen, J.-Y. Seo and N.-G. Park, *Adv. Energy Mater.*, 2018, **8**, 1702714.
16. K. T. Cho, G. Grancini, Y. Lee, E. Oveisi, J. Ryu, O. Almora, M. Tschumi, P. A. Schouwink, G. Seo, S. Heo, J. Park, J. Jang, S. Paek, G. Garcia-Belmonte and M. K. Nazeeruddin, *Energy Environ. Sci.*, 2018, **11**, 952-959.
17. K. T. Cho, Y. Zhang, S. Orlandi, M. Cavazzini, I. Zimmermann, A. Lesch, N. Tabet, G. Pozzi, G. Grancini and M. K. Nazeeruddin, *Nano Lett.*, 2018, **18**, 5467-5474.
18. I. García-Benito, C. Quarti, V. I. E. Queloz, S. Orlandi, I. Zimmermann, M. Cavazzini, A. Lesch, S. Marras, D. Beljonne, G. Pozzi, M. K. Nazeeruddin and G. Grancini, *Chem. Mater.*, 2018, **30**, 8211-8220.
19. G. Grancini, C. Roldán-Carmona, I. Zimmermann, E. Mosconi, X. Lee, D. Martineau, S. Narbey, F. Oswald, F. De Angelis, M. Graetzel and M. K. Nazeeruddin, *Nature Communications*, 2017, **8**, 15684.
20. Y. Bai, S. Xiao, C. Hu, T. Zhang, X. Meng, H. Lin, Y. Yang and S. Yang, *Adv. Energy Mater.*, 2017, **7**, 1701038.
21. T. M. Koh, V. Shanmugam, X. Guo, S. S. Lim, O. Filonik, E. M. Herzig, P. Müller-Buschbaum, V. Swamy, S. T. Chien, S. G. Mhaisalkar and N. Mathews, *J. Mater. Chem. A*, 2018, **6**, 2122-2128.
22. G. Grancini and M. K. Nazeeruddin, *Nat. Rev. Mater.*, 2019, **4**, 4-22.
23. C. Ortiz-Cervantes, P. Carmona-Monroy and D. Solis-Ibarra, *ChemSusChem*, 2019, **12**, 1560-1575.
24. B. Roose, A. Ummadisingu, J.-P. Correa-Baena, M. Saliba, A. Hagfeldt, M. Graetzel, U. Steiner and A. Abate, *Nano Energy*, 2017, **39**, 24-29.
25. J. M. Azpiroz, E. Mosconi, J. Bisquert and F. De Angelis, *Energy Environ. Sci.*, 2015, **8**, 2118-2127.
26. D. Meggiolaro, E. Mosconi and F. De Angelis, *ACS Energy Lett.*, 2019, **4**, 779-785.
27. Y. Yuan and J. Huang, *Acc. Chem. Res.*, 2016, **49**, 286-293.
28. M. E. F. Bouduban, V. I. E. Queloz, V. M. Caselli, K. T. Cho, A. R. Kirmani, S. Paek, C. Roldan-Carmona, L. J. Richter, J. E. Moser, T. J. Savenije, M. K. Nazeeruddin and G. Grancini, *J. Phys. Chem. Lett.*, 2019, **10**, 5713-5720.
29. S. R. Cowan, A. Roy and A. J. Heeger, *Phys. Rev. B*, 2010, **82**, 245207.
30. Z. Liu, S. Niu and N. Wang, *J. Colloid Interface Sci.*, 2018, **509**, 171-177.
31. K. Domanski, J.-P. Correa-Baena, N. Mine, M. K. Nazeeruddin, A. Abate, M. Saliba, W. Tress, A. Hagfeldt and M. Grätzel, *ACS Nano*, 2016, **10**, 6306-6314.

